Electronic Supplementary Material (ESI) for J. Mater. Chem. C

Intermolecular Hydrogen Bond induce Restriction of Access to Dark State for Triggering Aggregation-Induced Emission

Longjie Wang,‡[a] Yu Qin, ‡[b] Yi Cheng,[a] Wenwen Fan,[a] Shaoxiong Yang,[a] Liyan Zheng,*[a] and Qiue Cao*[a]

a.Key Laboratory of Medicinal Chemistry for Natural Resource, Ministry of Education. Yunnan Provincial Center for Research & Development of Natural Products. School of Chemical Science and Technology, Yunnan University, No. 2 North Cuihu Road, Kunming, 650091 (P.R. China)
b.Pharmacy College, Chongqing Engineering Research Center of Pharmaceutical Sciences, Chongqing Medical and Pharmaceutical College, Chongqing, China 401331
‡ These authors contributed equally to this work.

Materials

All chemicals and reagents are purchased from the market and supplied by Aladdin Company. The final products used in all experiments were purified on the silica gel column and recrystallized at least twice.

Measurement

^{1}H, ^{13}C-NMR spectra were recorded on AVANCE DRX 400 spectrometer (Bruker, German). HPLC-MS ware measured by electrospray ionization mass spectra were obtained with a High Performance 1100 Liquid Chromatography-Mass Spectrometer (Agilent Technologies, USA). A C18 column (250 mm* 4.6 mm, 5 μm, Hypersil GOLD, USA) was deployed as stationary phase. Digital photos were taken with the iPhone XR smartphone. Single-crystal X-ray diffraction (XRD) data were collected on a Rigaku Oxford Diffraction Supernova with Atlas Diffractometer, and crystal structures were solved with Olex2. Fluorescence spectra in the range of 300-700 nm were recorded with the F-4700 fluorescence spectrophotometer (HITACHI, Japan) at room temperature. Fluorescence decay curves measured by 285 nm and 390 nm excitation from Nano LED lamp on Horiba Jobin Yvon Fluorolog-3 spectrofluorometer. Fluorescence spectra, phosphorescence spectra and fluorescence quantum yields were measured on Horiba Jobin Yvon Fluorolog-3 spectrofluorometer. The size of nanoparticles in the solution was determined by NanoBrook Omni (Bruker, USA).

Computational Details

All the compounds were fully optimized with the density functional theory (DFT) in gaussian 09 method by using ω-b97xd density functional and Def2-TZVP basis set.[1] The SMD implicit solvation model is used to simulate the effect of solvent molecules on molecular properties through dielectric constant refraction. The natural transition orbits of excited electrons are analyzed by using Multiwfn and VMD programs.[2] The Hirshfeld surfaces and decomposed fingerprint plots were calculated and mapped using CrystalExplorer 17.5 package.[3] Single crystal analysis by olex2 software.[4]

Compounds Synthesis Method

1-(4-(quinolin-8-yl) phenyl) ethan-1-one (QLP-8)

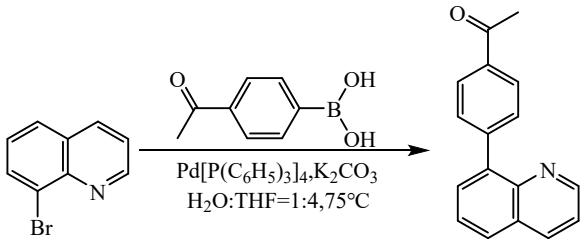

8-bromoquinoline (5.00 mmol, 1.0300 g) and (4-acetyl phenyl) boronic acid (7.00 mmol, 1.1480 g) were added into a 100.0 mL two-necked flask with 20.0 ml THF, potassium carbonate (0.5000 g, 3.62 mmol) were dissolved in 5.0 mL water (V_{THF}: V_{H_2O} = 4:1), mixed two solutions then add (0.10 mmol, 0.1156 g) (beta-4)-platinum. After stirring at 75 ℃ for 48 h under nitrogen gas, the reaction mixture was diluted with water and extracted with ethyl acetate. The organic layer was separated, washed with water and brine, dried with enough anhydrous sodium sulphate. After filtration, the filtrate was evaporated under reduced pressure and the crude product was purified on a silica gel column using petroleum/ether ethyl acetate (10/1, v/v) as eluent. 0.9900 g of QLP-8 was obtained as a colorless powder with 80.0% yield. The single crystal was obtained by recrystallization from the mixed solution of ethanol and water. ^{1}H NMR (400 MHz, Chloroform-*d*) δ(ppm): 8.95 (dd, *J* = 4.2, 1.8 Hz, 1H), 8.23 (dd, *J* = 8.3, 1.8 Hz, 1H), 8.12 – 8.02 (m, 2H), 7.87 (dd, *J* = 8.1, 1.5 Hz, 1H), 7.84 – 7.78 (m, 2H), 7.78 – 7.68 (m, 1H), 7.63 (dd, *J* = 8.1, 7.2 Hz, 1H), 7.44 (dd, *J* = 8.3, 4.2 Hz, 1H), 2.66 (s, 3H). ^{13}C NMR (400 MHz, Chloroform-*d*), δ(ppm): 198.02, 150.50, 144.59, 144.36, 139.72, 136.63, 136.43, 135.94, 130.91, 130.36, 128.80, 128.38, 128.09, 126.32, 121.28, 77.27, 26.74. HRMS: m/z: calculated for $C_{17}H_{13}NO$:247.0997; found: 270.0898 $[M+Na]^+$.

1-(4-(quinolin-5-yl) phenyl)ethan-1-one (QLP-5)

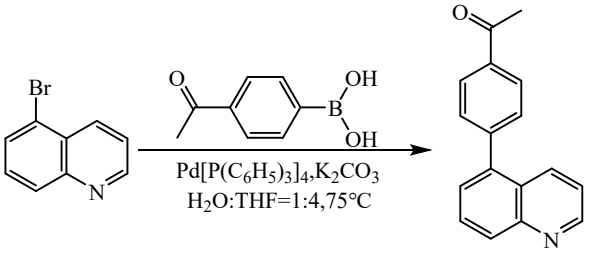

5-bromoquinoline (5.00 mmol, 1.0300 g) and (4-acetyl phenyl) boronic acid (7.00 mmol, 1.1480 g) were added into a 100.0 mL two-necked flask with 20.0 ml THF, potassium carbonate (0.5000 g, 3.62 mmol) were dissolved in 5.0 mL water (V_{THF}: V_{H_2O} = 4:1), mixed two solutions then add (0.10 mmol, 0.1156 g) (beta-4)-platinum. After stirring at 75 ℃ for 48 h under nitrogen gas, the reaction mixture was diluted with water and extracted with ethyl acetate. The organic layer was separated, washed with water and brine, dried with enough anhydrous sodium sulphate. After filtration, the filtrate was evaporated under reduced pressure and the crude product was purified on a silica gel column using petroleum/ether ethyl acetate (5/1, v/v) as eluent. 1.0100 g of QLP-5 was obtained as colorless powder with 82.3% yield. The pure powder was dissolved in a mixture of ethyl acetate and *n*-hexane and evaporated slowly for one week to obtain single crystal. ^{1}H NMR (400 MHz, Chloroform-*d*) δ(ppm): 8.95 (dd, *J* = 4.2, 1.7 Hz, 1H), 8.23 – 8.14 (m, 2H), 8.14 – 8.07 (m, 2H), 7.78 (dd, *J* = 8.5, 7.1 Hz, 1H), 7.61 – 7.55 (m, 2H), 7.52 (dd, *J* = 7.1, 1.2 Hz, 1H), 7.38 (dd, *J* = 8.6, 4.2 Hz, 1H), 2.69 (s, 3H). ^{13}C NMR (400 MHz, Chloroform-*d*) δ(ppm)： 197.68, 150.45, 148.49, 144.27,

139.27, 136.38, 133.94, 130.31, 129.72, 128.95, 128.55, 127.35, 126.39, 121.38, 77.28, 26.73. HRMS: m/z: calculated for $C_{17}H_{13}NO$:247.0997; found: 270.0893 $[M+Na]^+$.

1-(4-(isoquinolin-5-yl)phenyl)ethan-1-one (IQL-5)

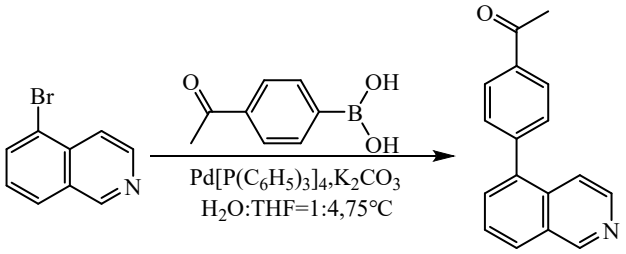

5-bromoisoquinoline (5.00 mmol, 1.0300 g) and (4-acetyl phenyl) boronic acid (7.00 mmol, 1.1480 g) were added into a 100.0 mL two-necked flask with 20.0 ml THF, potassium carbonate (0.5000 g, 3.62 mmol) were dissolved in 5.0 mL water (V_{THF}: V_{H_2O} = 4:1), mixed two solutions then add (0.10 mmol, 0.1156 g) (beta-4)-platinum. After stirring at 75 ℃ for 48 h under nitrogen gas, the reaction mixture was diluted with water and extracted with ethyl acetate. The organic layer was separated, washed with water and brine, dried with enough anhydrous sodium sulphate. After filtration, the filtrate was evaporated under reduced pressure and the crude product was purified on a silica gel column using petroleum/ether ethyl acetate (10/1, v/v) as eluent. 0.9800 g of IQL-5 was obtained as colorless powder with 78.9% yield. The pure powder was dissolved in a mixture of ethyl acetate and *n*-hexane and evaporated slowly for three days to obtain single crystal. ^{1}H NMR (400 MHz, Chloroform-*d*) δ(ppm): 9.34 (s, 1H), 8.52 (d, *J* = 6.0 Hz, 1H), 8.12 (d, *J* = 7.8 Hz, 2H), 8.04 (dd, *J* = 6.7, 2.7 Hz, 1H), 7.74 – 7.65 (m, 3H), 7.60 (d, *J* = 8.6 Hz, 2H), 2.75 (s, 0H), 2.70 (s, 3H). ^{13}C NMR (400 MHz, Chloroform-*d*) δ(ppm): 197.71, 152.98, 143.90, 143.63, 138.01, 136.42, 133.79, 131.02, 130.16, 128.91, 128.63, 127.95, 126.87, 118.15, 77.24, 26.76. $C_{17}H_{13}NO$:247.0997; found: 270.0872$[M+Na]^+$.

1-(4-(benzo[c] [1,2,5] thiadiazol-4-yl) phenyl) ethan-1-one (BTD-4)

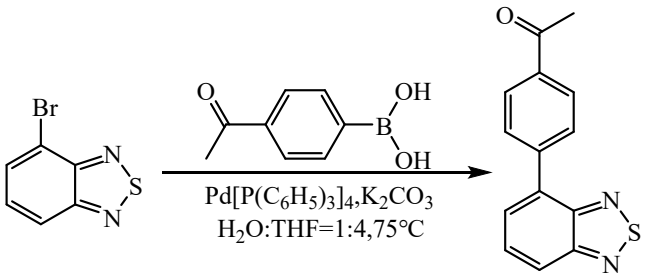

4-bromobenzo[c] [1,2,5] thiadiazole (5.00 mmol, 1.0700 g) and (4-acetyl phenyl) boronic acid (7.00 mmol, 1.1480 g) were added into a 100.0 mL two-necked flask with 20.0 ml THF, potassium carbonate (0.5000 g, 3.62 mmol) were dissolved in 5.0 mL water (V_{THF}: V_{H_2O} = 4:1), mixed two

solutions then add (0.10 mmol, 0.1156 g) (beta-4)-platinum. After stirring at 75 ℃ for 48 h under nitrogen gas, the reaction mixture was diluted with water and extracted with ethyl acetate. The organic layer was separated, washed with water and brine, dried with enough anhydrous sodium sulphate. After filtration, the filtrate was evaporated under reduced pressure and the crude product was purified on a silica gel column using petroleum/ether ethyl acetate (20/1, v/v) as eluent. 0.6400 g of BTD-4 was obtained as green powder with 54.0% yield. The pure powder was dissolved in a mixture of ethyl acetate and n-hexane and evaporated slowly for two days to obtain single crystal. ^{1}H NMR (400 MHz, Chloroform-*d*) δ 8.12 (d, *J* = 6.5 Hz, 1H), 8.11 (s, 1H), 8.06 (d, *J* = 4.5 Hz, 2H), 8.04 – 8.02 (m, 1H), 7.77 – 7.68 (m, 2H), 2.67 (s, 3H). ^{13}C NMR (400 MHz, Chloroform-*d*) δ 197.67, 155.56, 141.88, 133.27, 129.48, 128.60, 128.24, 121.49, 77.24, 26.72. $C_{14}H_{10}N_2OS$:254.0514; found: 255.0592 $[M+H]^+$.

1-(4-(naphthalen-1-yl) phenyl) ethan-1-one (NTP-1)

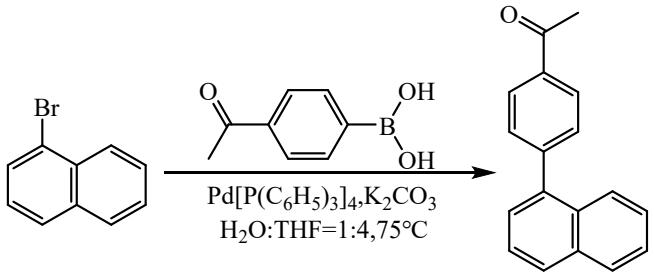

1-bromonaphthalene (5.00 mmol, 1.0500 g) and (4-acetyl phenyl) boronic acid (7.00 mmol, 1.1480 g) were added into a 100.0 mL two-necked flask with 20.0 ml THF, potassium carbonate (0.5000 g, 3.62 mmol) were dissolved in 5.0 mL water (V_{THF}: V_{H_2O} = 4:1), mixed two solutions then add (0.10 mmol, 0.1156 g) (beta-4)-platinum. After stirring at 75 ℃ for 48 h under nitrogen gas, the reaction mixture was diluted with water and extracted with ethyl acetate. The organic layer was separated, washed with water and brine, dried with enough anhydrous sodium sulphate. After filtration, the filtrate was evaporated under reduced pressure and the crude product was purified on a silica gel column using petroleum/ether ethyl acetate (50/1, v/v) as eluent. 1.0200 g of NTP-1 was obtained as colorless powder with 82.3% yield. ^{1}H NMR (400 MHz, Chloroform-*d*) δ(ppm): 8.09 (d, *J* = 8.4 Hz, 2H), 7.91 (t, *J* = 9.7 Hz, 2H), 7.84 (d, *J* = 8.4 Hz, 1H), 7.61 (d, *J* = 6.4 Hz, 2H), 7.53 (dt, *J* = 11.7, 7.6 Hz, 2H), 7.47 – 7.41 (m, 2H), 2.69 (s, 3H). ^{13}C NMR (400 MHz, Chloroform-*d*) δ(ppm): 197.90, 145.82, 139.03, 136.00, 133.80, 131.21, 130.34, 128.45, 128.39, 128.38, 126.95, 126.41, 126.03, 125.58, 125.37, 26.75. $C_{18}H_{14}O$:246.1045; found: 247.1127 $[M+H]^+$.

4-(quinolin-5-yl) benzaldehyde (QLB-8)

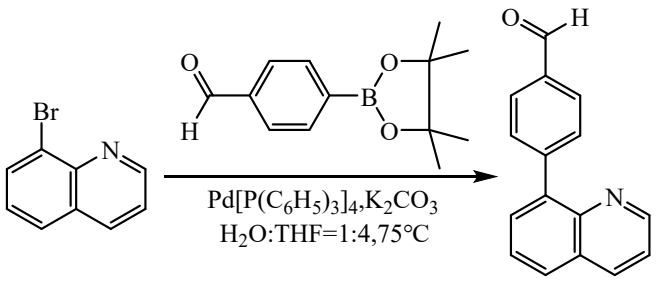

4-(4,4,5,5-tetramethyl-1,3,2-dioxaborolan-2-yl) benzaldehyde (7.00 mmol, 1.6250 g) and 8-bromoquinoline (5.00 mmol, 1.0300 g) and were added into a 100.0 mL two-necked flask with 20.0 ml THF, potassium carbonate (0.5000 g, 3.62 mmol) were dissolved in 5.0 mL water (V_{THF}: V_{H_2O} = 4:1), mixed two solutions then add (0.10 mmol, 0.1156 g) (beta-4)-platinum. After stirring at 75 ℃ for 48 h under nitrogen gas, the reaction mixture was diluted with water and extracted with ethyl acetate. The organic layer was separated, washed with water and brine, dried with enough anhydrous sodium sulphate. After filtration, the filtrate was evaporated under reduced pressure and the crude product was purified on a silica gel column using petroleum/ether ethyl acetate (3/1, v/v) as eluent. 0.9900 g of QLB-8 was obtained as colorless powder with 85.0% yield. Crystals are obtained by recrystallization of pure powders using ethanol and water as mixed solvents. ^{1}H NMR (400 MHz, Chloroform-*d*) δ(ppm): 10.10 (s, 1H), 8.96 – 8.95 (m, 1H), 8.24 (d, *J* = 6.5 Hz, 1H), 8.01 (d, *J* = 6.0 Hz, 2H), 7.89 (d, *J* = 3.1 Hz, 3H), 7.76 (d, *J* = 5.6 Hz, 1H), 7.64 (d, *J* = 1.1 Hz, 1H), 7.45 (d, *J* = 4.2 Hz, 1H). ^{13}C NMR (400 MHz, Chloroform-*d*) δ(ppm): 192.26, 150.56, 146.04, 145.74, 139.49, 136.44, 135.23, 131.37, 130.38, 129.44, 128.78, 128.59, 126.32, 121.36. $C_{16}H_{11}NO$:233.0841; found: 234.0932 $[M+H]^+$.

Nuclear Magnetic Resonance (NMR) Spectra

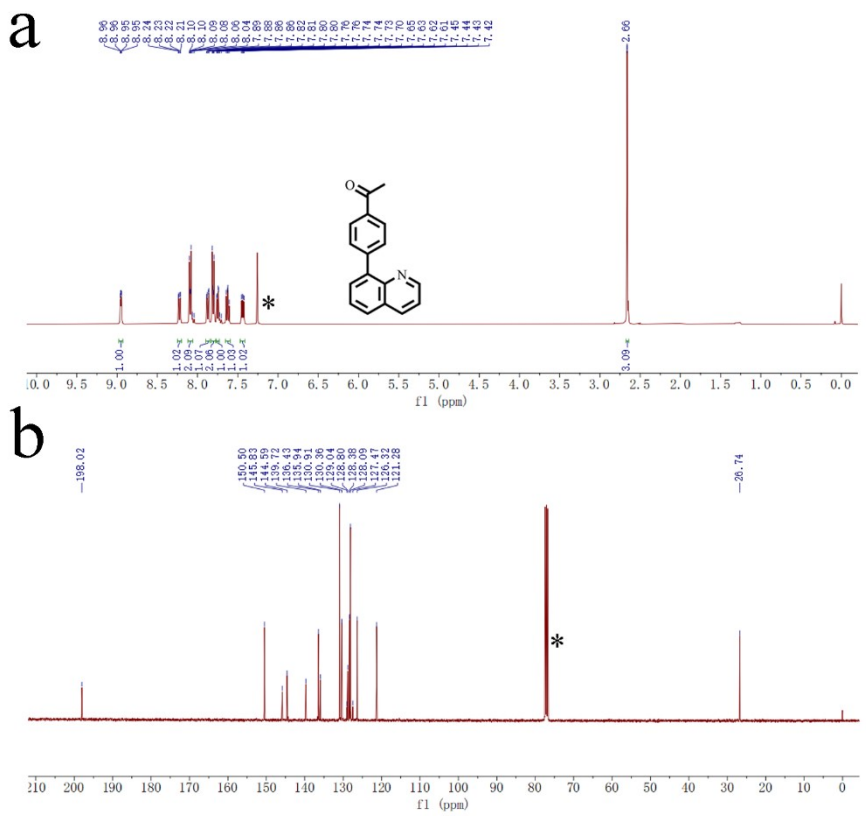

Figure S1. **a** ^{1}H and **b** ^{13}C NMR spectra of QLP-8. The solvent peaks were marked as asterisk.

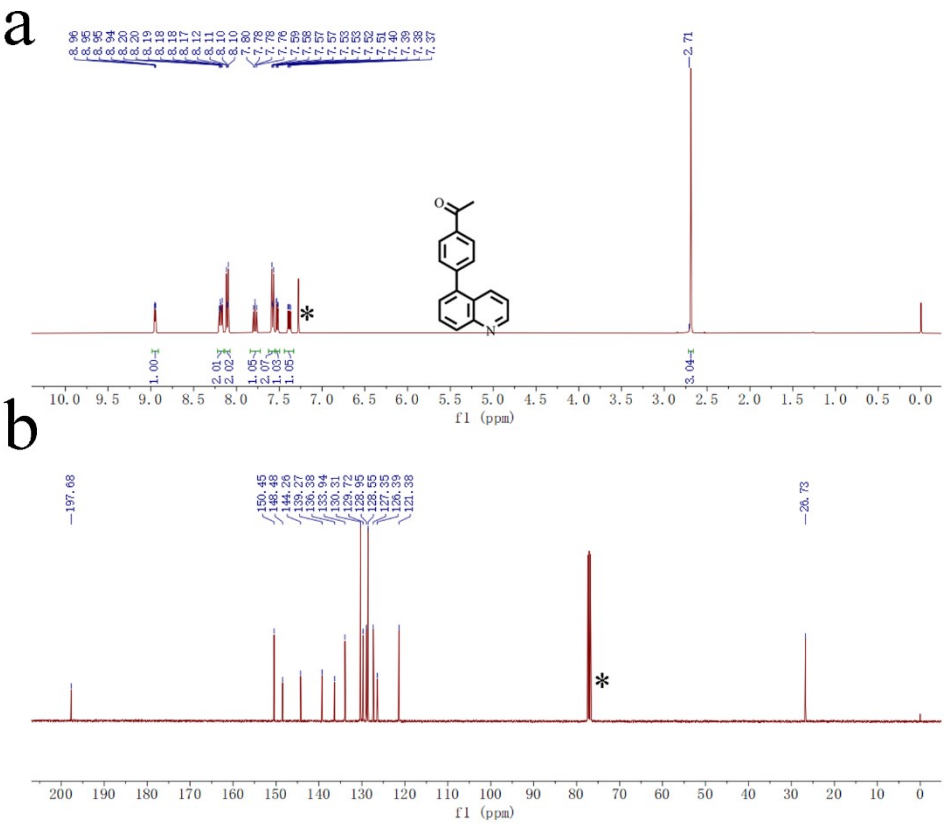

Figure S2. **a** ^{1}H and **b** ^{13}C NMR spectra of QLP-5. The solvent peaks were marked as asterisk.

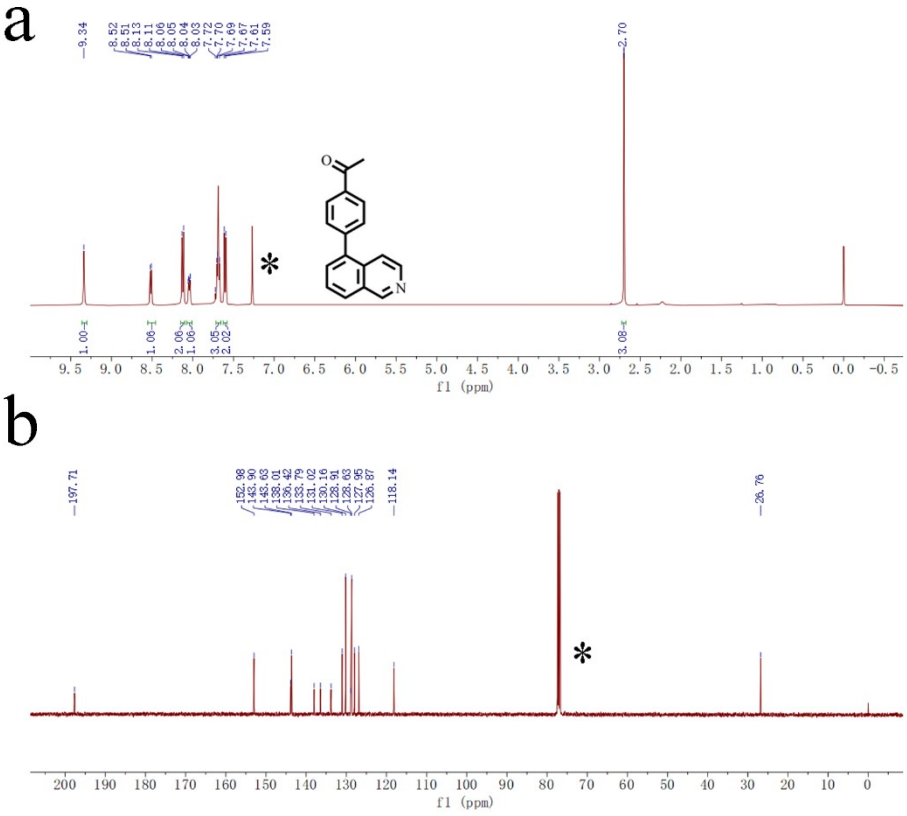

Figure S3. **a** ^{1}H and **b** ^{13}C NMR spectra of IQL-5. The solvent peaks were marked as asterisk.

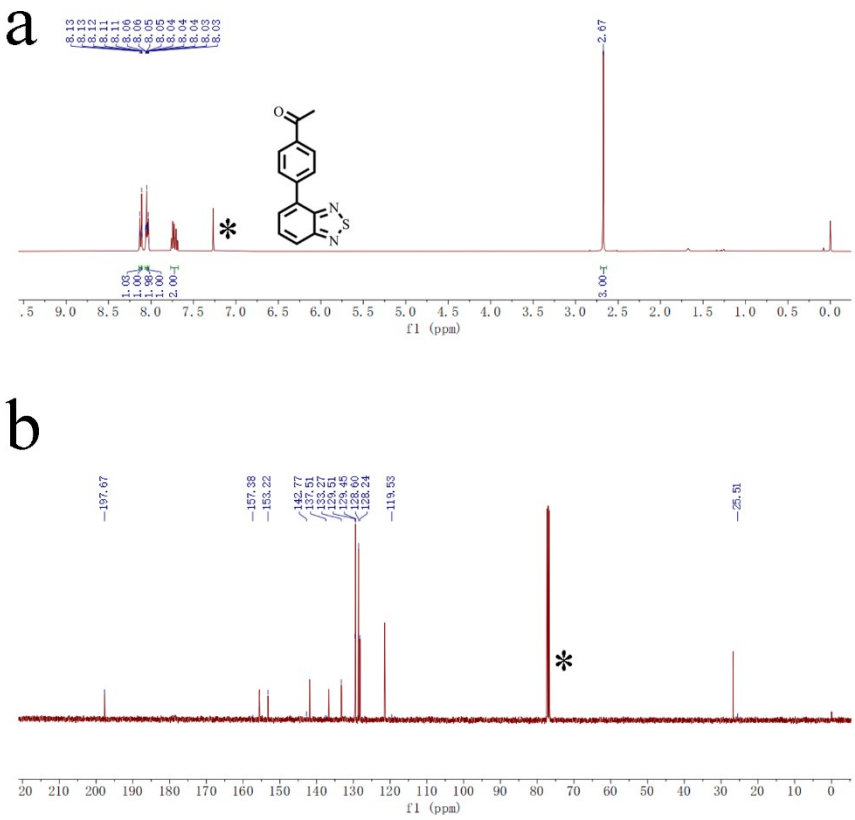

Figure S4. a ^{1}H and **b** ^{13}C NMR spectra of BTD-4. The solvent peaks were marked as asterisk.

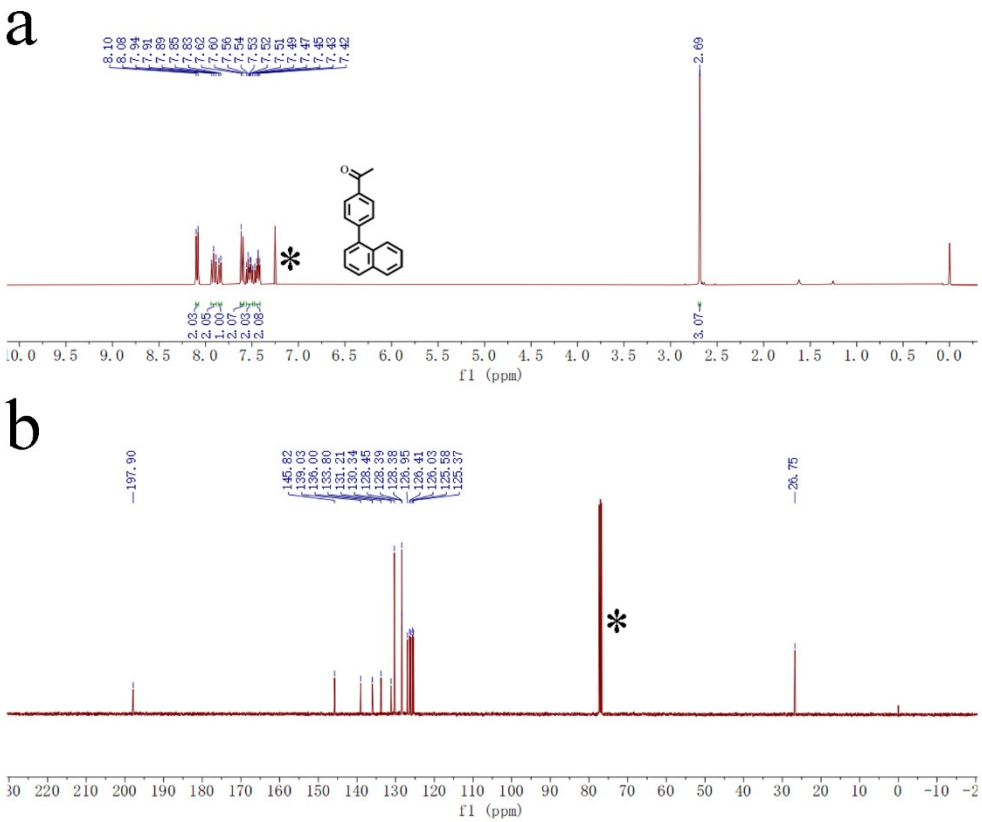

Figure S5. a ^{1}H and **b** ^{13}C NMR spectra of NTP-1. The solvent peaks were marked as asterisk.

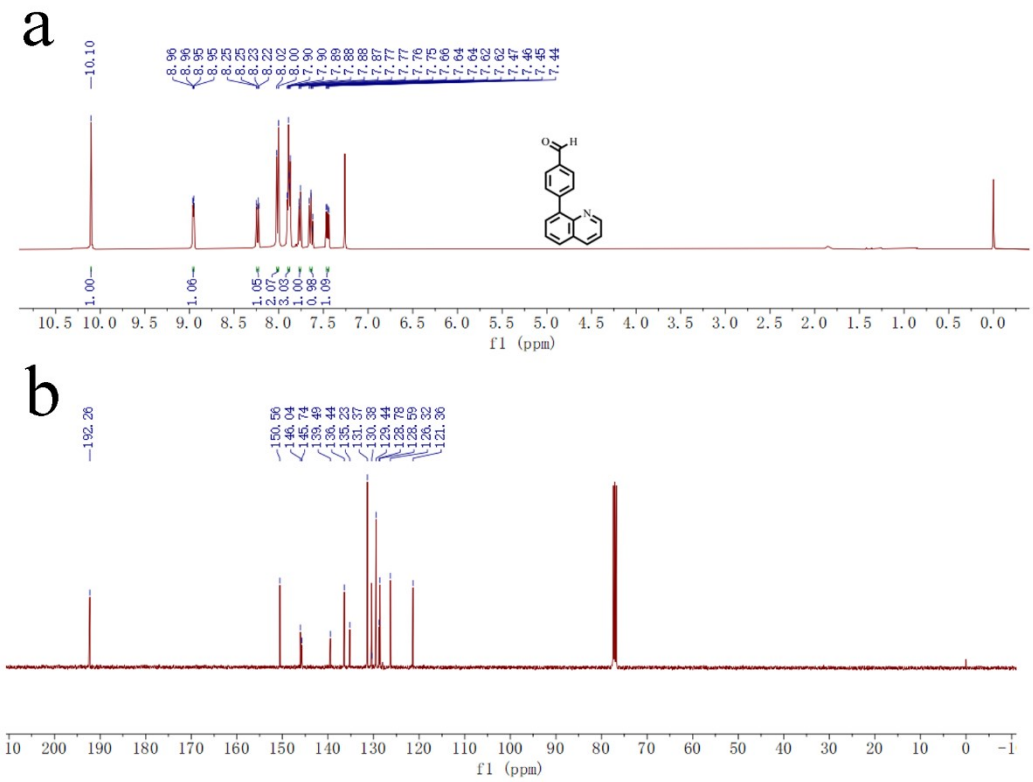

Figure S6. a ^{1}H and **b** ^{13}C NMR spectra of QLB-8 the solvent peaks were marked as asterisk.

High Resolution Mass Spectrometry

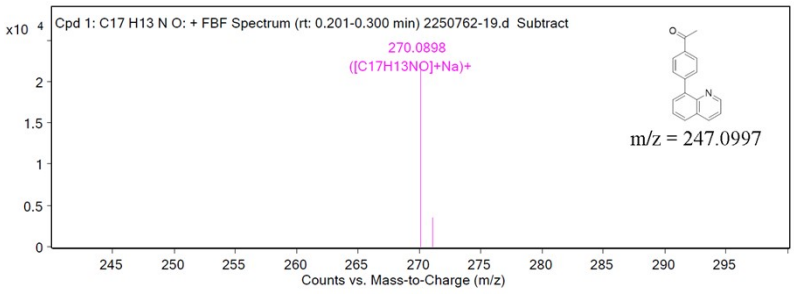

Figure S7. High resolution mass spectrum of QLP-8 with chemical ionization.

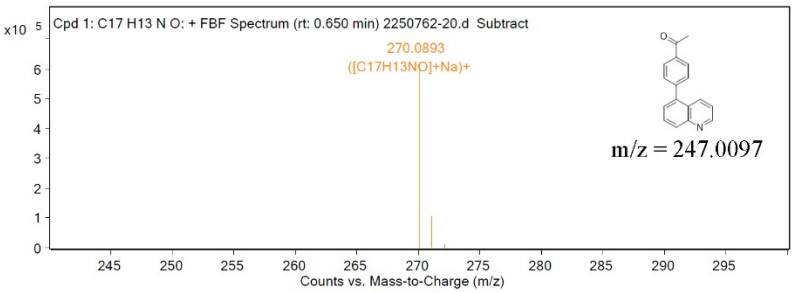

Figure S8. High resolution mass spectrum of QLP-5 with chemical ionization.

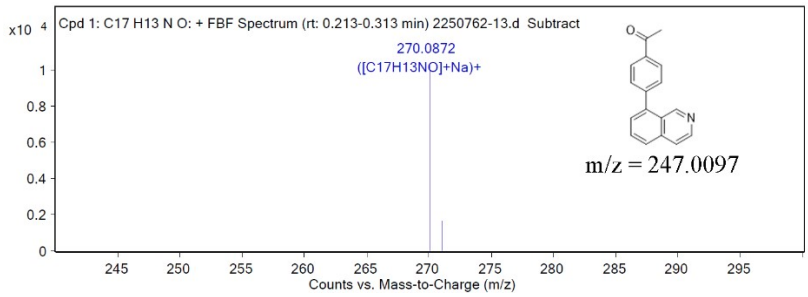

Figure S9. High resolution mass spectrum of IQL-5 with chemical ionization.

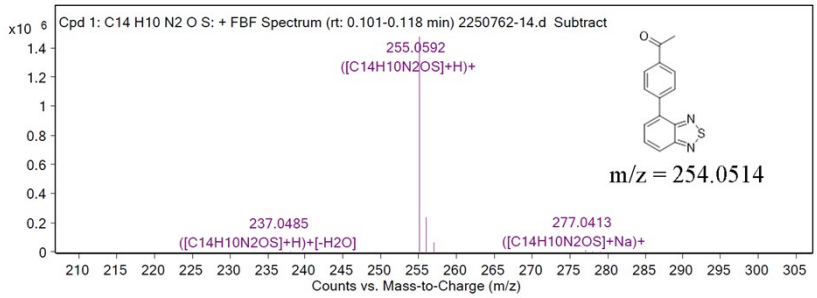

Figure S10. High resolution mass spectrum of BTD-4 with chemical ionization.

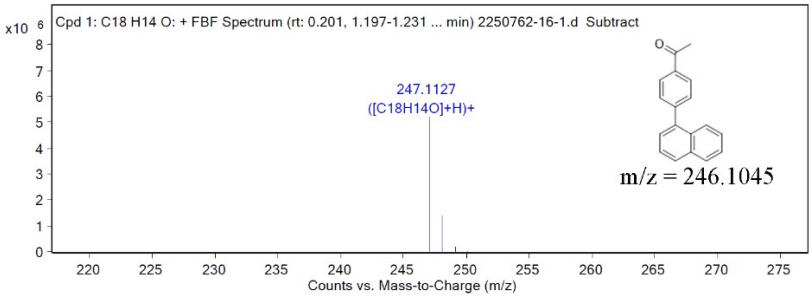

Figure S11. High resolution mass spectrum of NTP-1 with chemical ionization.

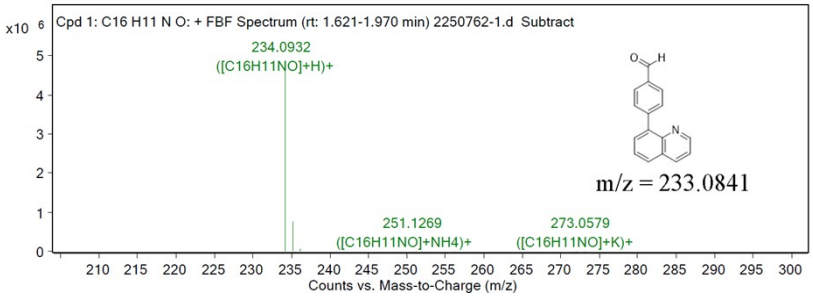

Figure S12. High resolution mass spectrum of QLB-8 with chemical ionization.

Size Distribution

Table S1. The size distribution of QLP-8 in the different solvent systems. Concentration = 10^{-5} M.

	particle size (nm)	Polydispersity
V_{H_2O} : V_{THF} = 7:3	356.3	0.047
V_{H_2O} : V_{THF} = 8:2	881.5	0.031
V_{H_2O} : V_{THF} = 9:1	1431.5	0.024
$V_{n\text{-hexane}}$: V_{THF} = 9:1	989.9	0.065
V_{D_2O} : V_{THF} = 9:1	1123.5	0.076

Table S2. The size distribution of QLP-5 in the different solvent systems. Concentration = 10^{-5} M.

	particle size (nm)	Polydispersity
V_{H_2O} : V_{THF} = 7:3	298.5	0.048
V_{H_2O} : V_{THF} = 8:2	688.7	0.078
V_{H_2O} : V_{THF} = 9:1	998.2	0.005
$V_{n\text{-hexane}}$: V_{THF} = 9:1	889.3	0.031
V_{D_2O} : V_{THF} = 9:1	989.8	0.088

Table S3. The size distribution of IQL-5 in the different solvent systems. Concentration = 10^{-5} M.

	particle size (nm)	Polydispersity
V_{H_2O} : V_{THF} = 7:3	332.7	0.077
V_{H_2O} : V_{THF} = 8:2	858.6	0.004
V_{H_2O} : V_{THF} = 9:1	1323.5	0.032
$V_{n\text{-hexane}}$: V_{THF} = 9:1	969.5	0.029
V_{D_2O} : V_{THF} = 9:1	1003.2	0.058

Table S4. The size distribution of BTD-4 in the different solvent systems. Concentration = 10^{-5} M.

	particle size (nm)	Polydispersity
V_{H_2O} : V_{THF} = 7:3	199.8	0.023
V_{H_2O} : V_{THF} = 8:2	458.6	0.088
V_{H_2O} : V_{THF} = 9:1	887.2	0.046
$V_{n\text{-hexane}}$: V_{THF} = 9:1	677.4	0.084
V_{D_2O} : V_{THF} = 9:1	798.5	0.057

Table S5. The size distribution of NTP-1 in the different solvent systems. Concentration = 10^{-5} M.

	particle size (nm)	Polydispersity
V_{H_2O} : V_{THF} = 7:3	488.7	0.102
V_{H_2O} : V_{THF} = 8:2	996.1	0.125
V_{H_2O} : V_{THF} = 9:1	1835.6	0.166
$V_{n\text{-hexane}}$: V_{THF} = 9:1	1063.6	0.096
V_{D_2O} : V_{THF} = 9:1	1336.4	0.112

Table S6. The size distribution of QLB-8 in the different solvent systems. Concentration = 10^{-5} M.

	particle size (nm)	Polydispersity
V_{H_2O} : V_{THF} = 7:3	332.1	0.018
V_{H_2O} : V_{THF} = 8:2	554.4	0.022
V_{H_2O} : V_{THF} = 9:1	980.2	0.046
$V_{n\text{-hexane}}$: V_{THF} = 9:1	680.4	0.032
V_{D_2O} : V_{THF} = 9:1	798.8	0.042

Spectroscopic Data

UV-vis Absorption Spectra

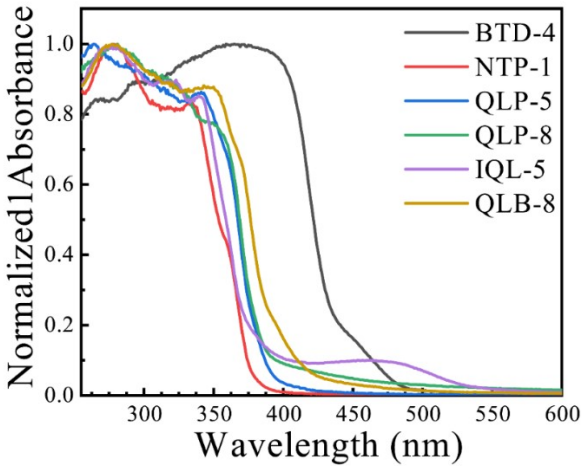

Figure S13. The solid-state UV-vis absorption spectra of compounds.

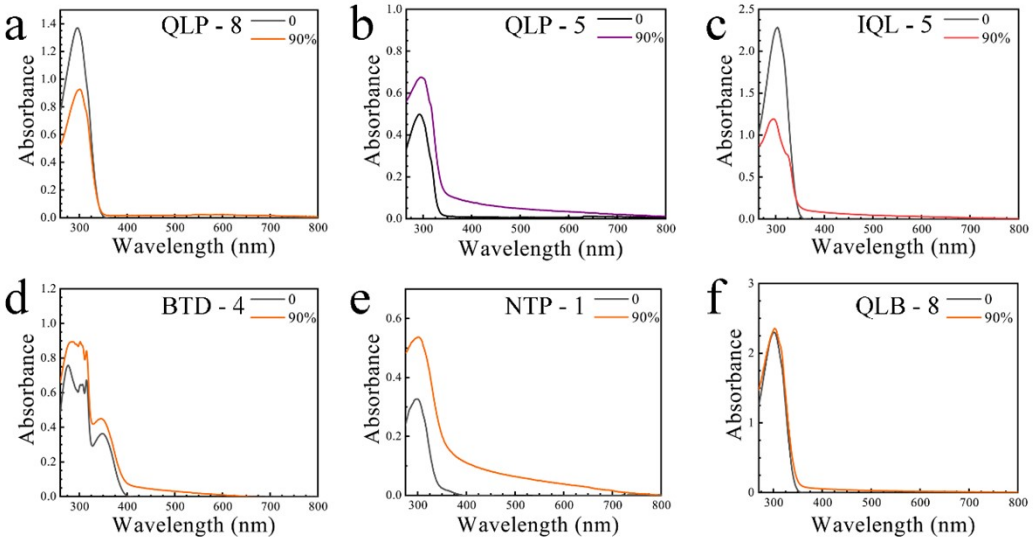

Figure S14. a-f The UV-vis absorption spectra of compounds in different water fraction.

Solid State Excitation and Emission Spectra

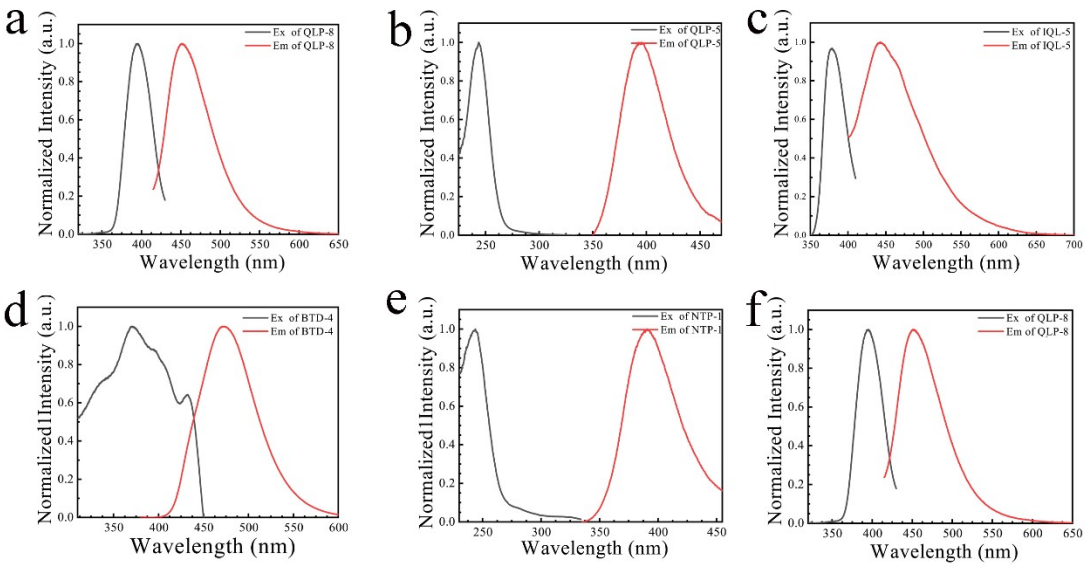

Figure S15. The solid-state excitation and emission wavelength of compounds.

Fluorescence Lifetime and Quantum Yield.

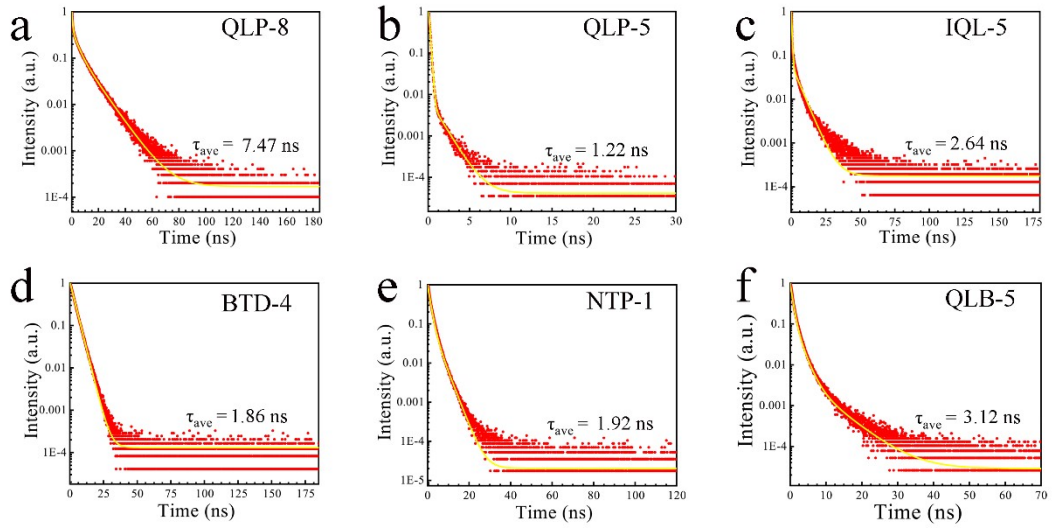

Figure S16. The solid-state fluorescence lifetime of compounds.

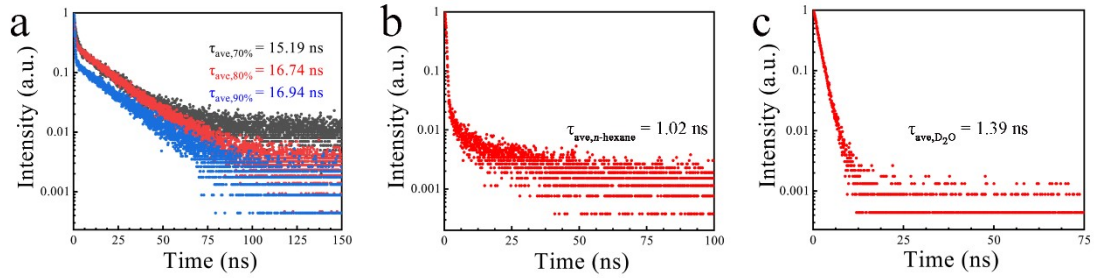

Figure S17. a. The lifetime of QLP-8 in different water fraction, **b** and **c** lifetime of QLP-8 use *n*-hexane and D_2O as poor solvent (the poor solvent volume ratio = 90%).

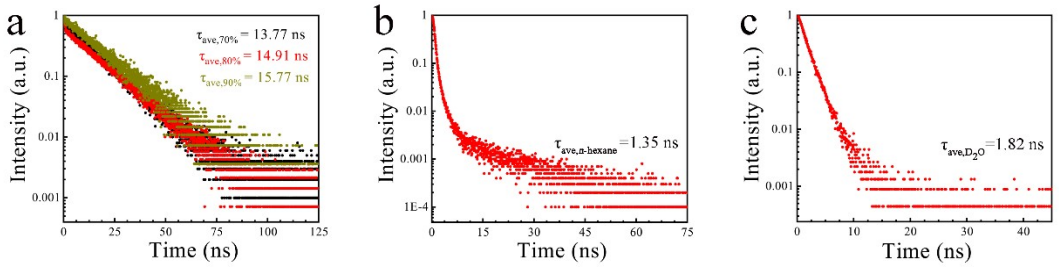

Figure S18. a. The lifetime of QLP-5 in different water fraction, **b** and **c** lifetime of QLP-5 use *n*-hexane and D_2O as poor solvent (the poor solvent volume ratio = 90%).

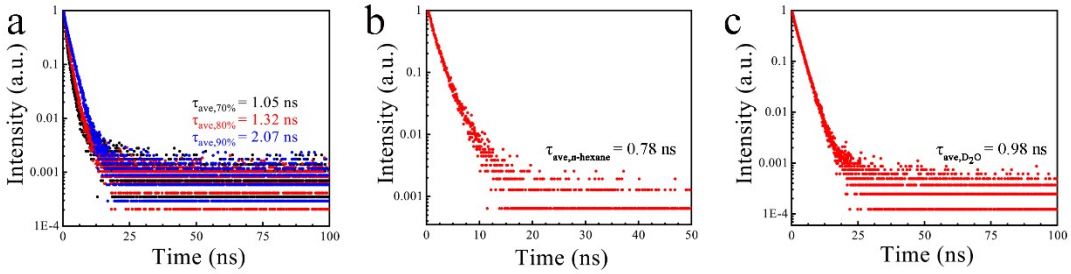

Figure S19. a. The lifetime of IQL-5 in different water fraction, **b** and **c** lifetime of IQL-5 use *n*-hexane and D_2O as poor solvent (the poor solvent volume ratio = 90%).

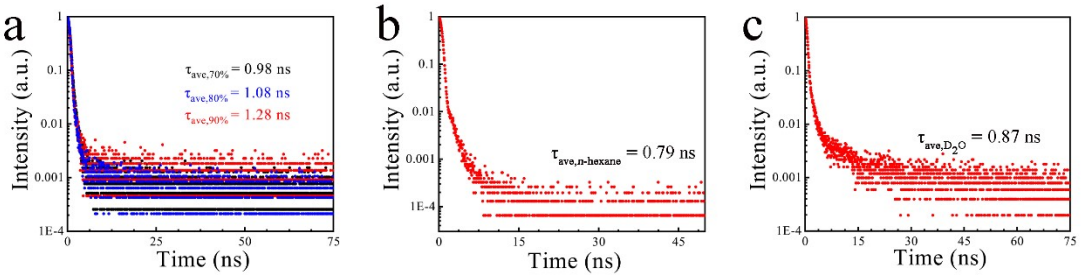

Figure S20. a. The lifetime of BTD-4 in different water fraction, **b** and **c** lifetime of BTD-4 use *n*-hexane and D_2O as poor solvent (the poor solvent volume ratio = 90%).

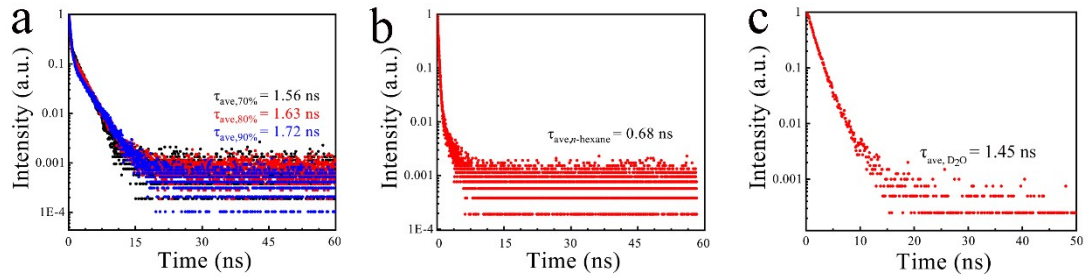

Figure S21. a. The lifetime of NTP-1 in different water fraction, **b** and **c** lifetime of NTP-1 use *n*-hexane and D_2O as poor solvent (the poor solvent volume ratio = 90%).

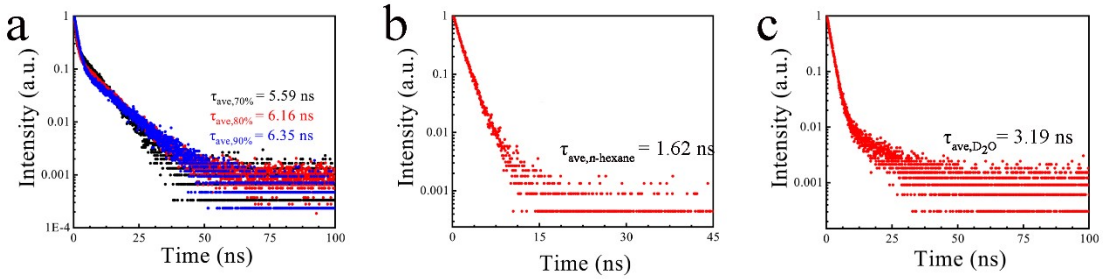

Figure S22. a. The lifetime of QLB-8 in different water fraction, **b** and **c** lifetime of QLB-8 use *n*-hexane and D_2O as poor solvent (the poor solvent volume ratio = 90%).

Table S7. The photophysical parameters of QLP-5. Φ_f = fluorescence quantum yield, k_r = radiative decay rate constant = Φ_f / τ_f, k_{nr} = nonradiative decay rate constant = $(1 - \Phi_f)/ \tau_f$, where τ_f = fluorescence lifetime.

	τ_f(ns)	Φ_f(%)	k_r (× 10^6 s^{-1})	k_{nr} (× 10^6 s^{-1})
V_{H_2O} : V_{THF} = 7:3	13.77	3.11	2.25	70.37
V_{H_2O} : V_{THF} = 8:2	14.91	6.32	4.23	62.84
V_{H_2O} : V_{THF} = 9:1	15.77	10.24	6.47	56.94
$V_{n\text{-hexane}}$: V_{THF} = 9:1	1.35	1.12	8.15	732.59
V_{D_2O} : V_{THF} = 9:1	1.82	4.21	23.08	526.37

Table S8. The photophysical parameters of IQL-5. Φ_f = fluorescence quantum yield, k_r = radiative decay rate constant = Φ_f / τ_f, k_{nr} = nonradiative decay rate constant = $(1 - \Phi_f)/\tau_f$, where τ_f = fluorescence lifetime.

	τ_f(ns)	Φ_f(%)	k_r (× 10^6 s^{-1})	k_{nr} (× 10^6 s^{-1})
V_{H_2O} : V_{THF} = 7:3	1.05	3.32	31.62	920.76
V_{H_2O} : V_{THF} = 8:2	1.32	8.56	64.85	692.73
V_{H_2O} : V_{THF} = 9:1	2.07	15.33	74.06	409.03
$V_{n\text{-hexane}}$: V_{THF} = 9:1	0.78	1.25	16.03	1266.03
V_{D_2O} : V_{THF} = 9:1	0.98	8.77	89.49	930.92

Table S9. The photophysical parameters of BTD-4. Φ_f = fluorescence quantum yield, k_r = radiative decay rate constant = Φ_f / τ_f, k_{nr} = nonradiative decay rate constant = $(1 - \Phi_f)/\tau_f$, where τ_f = fluorescence lifetime.

	τ_f(ns)	Φ_f(%)	k_r (× 10^6 s^{-1})	k_{nr} (× 10^6 s^{-1})
V_{H_2O} : V_{THF} = 7:3	0.98	20.77	211.94	808.47
V_{H_2O} : V_{THF} = 8:2	1.08	30.23	279.90	646.02
V_{H_2O} : V_{THF} = 9:1	1.28	42.2	329.68	451.56
$V_{n\text{-hexane}}$: V_{THF} = 9:1	0.79	18.88	238.99	1026.84
V_{D_2O} : V_{THF} = 9:1	0.87	35.33	406.09	743.33

Table S10. The photophysical parameters of NTP-1. Φ_f = fluorescence quantum yield, k_r = radiative decay rate constant = Φ_f / τ_f, k_{nr} = nonradiative decay rate constant = $(1 - \Phi_f)/\tau_f$, where τ_f =

fluorescence lifetime.

	τ_f(ns)	Φ_f(%)	k_r(× 10^6 s^{-1})	k_{nr} (× 10^6 s^{-1})
V_{H_2O} : V_{THF} = 7:3	1.56	1.98	12.69	628.33
V_{H_2O} : V_{THF} = 8:2	1.63	3.44	21.10	592.39
V_{H_2O} : V_{THF} = 9:1	1.72	6.77	39.36	542.03
$V_{n\text{-hexane}}$: V_{THF} = 9:1	0.68	1.11	16.32	1454.26
V_{D_2O} : V_{THF} = 9:1	1.45	4.88	33.66	656.00

Table S11. The photophysical parameters of QLB-8. Φ_f = fluorescence quantum yield, k_r = radiative decay rate constant = Φ_f /τ_f, k_{nr} = nonradiative decay rate constant = (1 - Φ_f)/τ_f, where τ_f = fluorescence lifetime.

	τ_f(ns)	Φ_f(%)	k_r(× 10^6 s^{-1})	k_{nr} (× 10^6 s^{-1})
V_{H_2O} : V_{THF} = 7:3	5.59	7.33	13.11	165.78
V_{H_2O} : V_{THF} = 8:2	6.16	18.58	30.16	132.18
V_{H_2O} : V_{THF} = 9:1	6.35	23.46	36.94	120.94
$V_{n\text{-hexane}}$: V_{THF} = 9:1	1.62	1.03	6.35	610.93
V_{D_2O} : V_{THF} = 9:1	3.19	15.35	48.11	265.36

Other spectral data

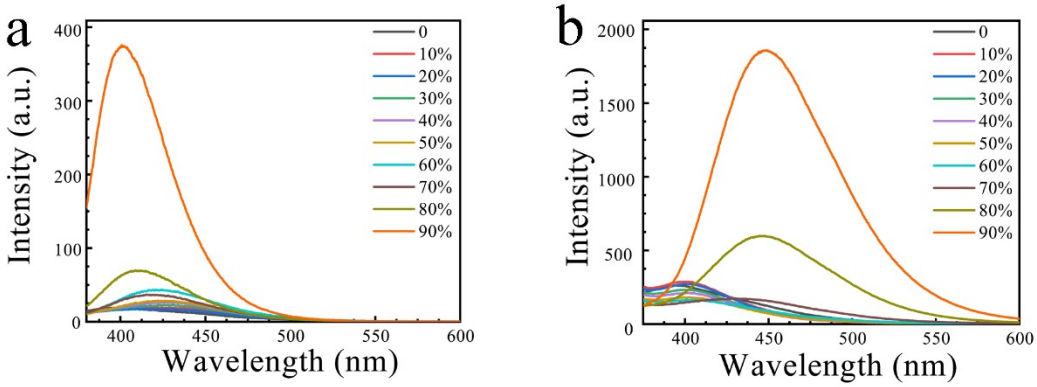

Figure S23. a. PL spectra of QLP-8 in *n*-hexane/THF mixtures with different *n*-hexane fractions. c = 10^{-5} M, λ_{ex} = 325 nm. **b.** PL spectra of QLP-8 in D_2O/THF mixtures with different D_2O fractions. c = 10^{-5} M, λ_{ex} = 345 nm.

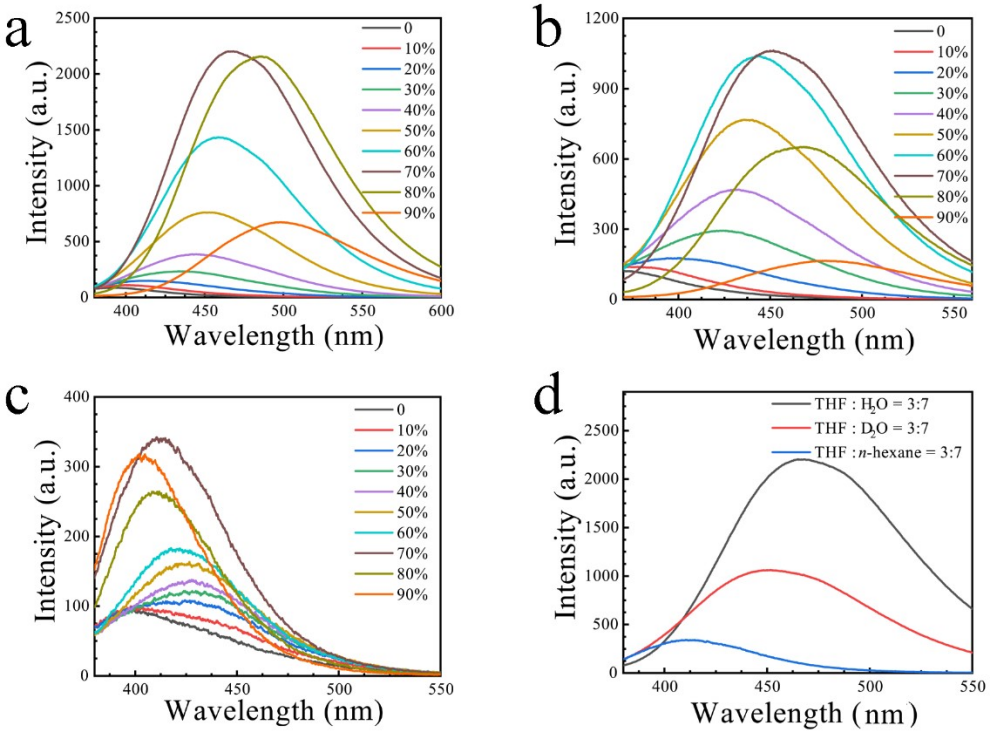

Figure S24. a. PL spectra of NTP-1 in H_2O/THF mixtures with different water fractions (*fw*). c = 10^{-5} M, λ_{ex} = 305 nm. **b**. PL spectra of NTP-1 in D_2O/THF mixtures with different D_2O fractions. c = 10^{-5} M, λ_{ex} = 325 nm. **c.** PL spectra of NTP-1 in *n*-hexane/THF mixtures with different *n*-hexane fractions. c = 10^{-5} M, λ_{ex} = 305 nm. **d.** PL spectra of NTP-1 in different poor solvent under the same condition.

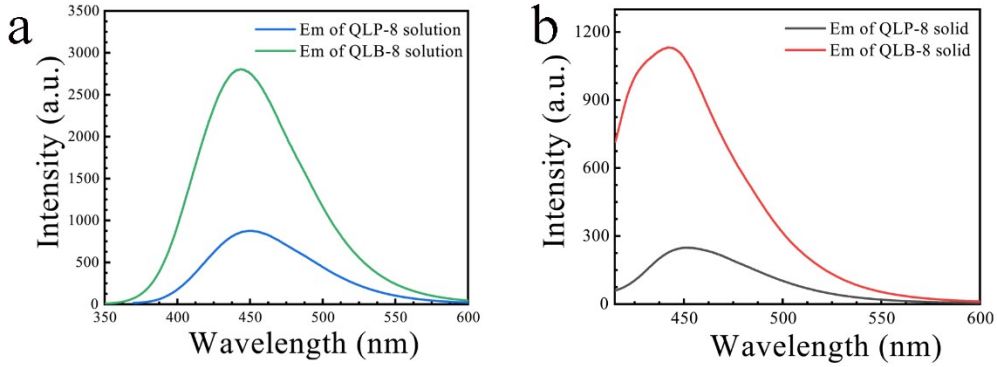

Figure S25. a. PL spectra of QLP-8 and QLB-8 in the solution with the concentration of 10^{-5} M, $\lambda_{ex,QLP-8}$ = 356.0 nm, $\lambda_{ex,QLB-8}$ = 370.0 nm. **b.** PL spectra of QLP-8 and QLB-8 in the solid state, $\lambda_{ex,QLP-8}$ = 395.0 nm, $\lambda_{ex,QLB-8}$ = 402.2 nm.

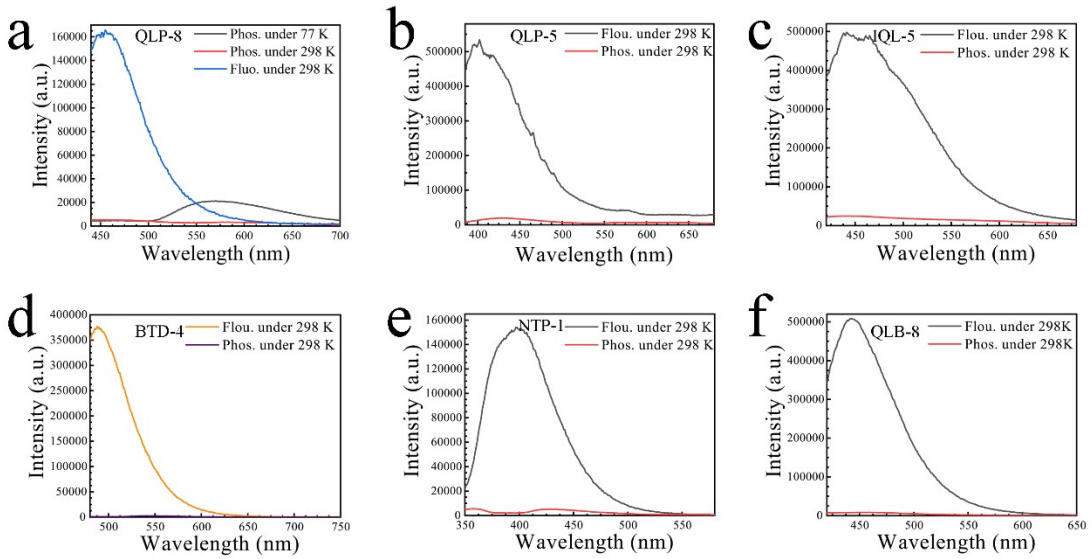

Figure S26. a-f The fluorescence spectra and phosphorescence spectra of compounds.

The Crystal Structure of Compounds.

Table S12. Summary of crystallographic data and structural refinements

Compound	QLP-8	QLP-5	IQL-5	BTD-4
CCDC number	2111659	2111734	2111661	2111663
Empirical formula	$C_{17}H_{13}NO$	$C_{17}H_{13}NO$	$C_{17}H_{13}NO$	$C_{14}H_{10}N_2OS$
Formula weight	247.28	247.28	247.28	254.30
Temperature/K	101(3)	301.08(10)	193.0	100.01(10)
Crystal system	triclinic	monoclinic	monoclinic	monoclinic
Space group	P-1	$P2_1/c$	$P2_1/c$	$P2_1/c$
a/Å	3.80620(10)	17.7346(3)	11.2612(10)	3.8241(2)
b/Å	12.7167(3)	14.1145(2)	7.3739(8)	21.5934(8)
c/Å	13.5789(2)	16.7364(3)	15.4845(15)	13.7628(5)
α/°	67.404(2)	90	90	90
β/°	87.172(2)	114.410(2)	92.600(4)	94.180(3)
γ/°	89.413(2)	90	90	90
Volume/Å^3	606.03(2)	3814.89(12)	1284.5(2)	1133.44(8)
Z	2	12	4	4
Density/ g.cm^{-3}	1.355	1.292	1.279	1.490
F (000)	260.0	1560.0	520.0	528.0
μ/mm^{-1}	0.665	0.633	0.080	0.272
Goodness-of-fit on F^2	1.074	1.036	1.017	528.0
R_1 [I>=2σ (I)][b]	0.0608	0.0508	0.0564	0.0408
wR_2 [I>=2σ (I)][c]	0.1583	0.1456	0.1169	0.1237
R_1 [all data] [b]	0.0625	0.0635	0.1044	0.0521

wR_2 [all data][c]	0.1595	0.1564	0.1433	0.1332

Compound	QLB-8
CCDC number	2111665
Empirical formula	$C_{16}H_{11}NO$
Formula weight	233.26
Temperature/K	300.92(10)
Crystal system	monoclinic
Space group	$P2_1/c$
a/Å	10.7848(8)
b/Å	7.4289(4)
c/Å	14.9066(9)
α/°	90
β/°	96.205(7)
γ/°	90
Volume/Å^3	1187.31(13)
Z	4
Density/ g.cm^{-3}	1.305
F (000)	488
μ/mm^{-1}	0.082
Goodness-of-fit on F^2	1.068
R_1 [I>=2σ (I)][b]	0.0444
wR_2 [I>=2σ (I)][c]	0.1107
R_1 [all data] [b]	0.0733
wR_2 [all data][c]	0.1241

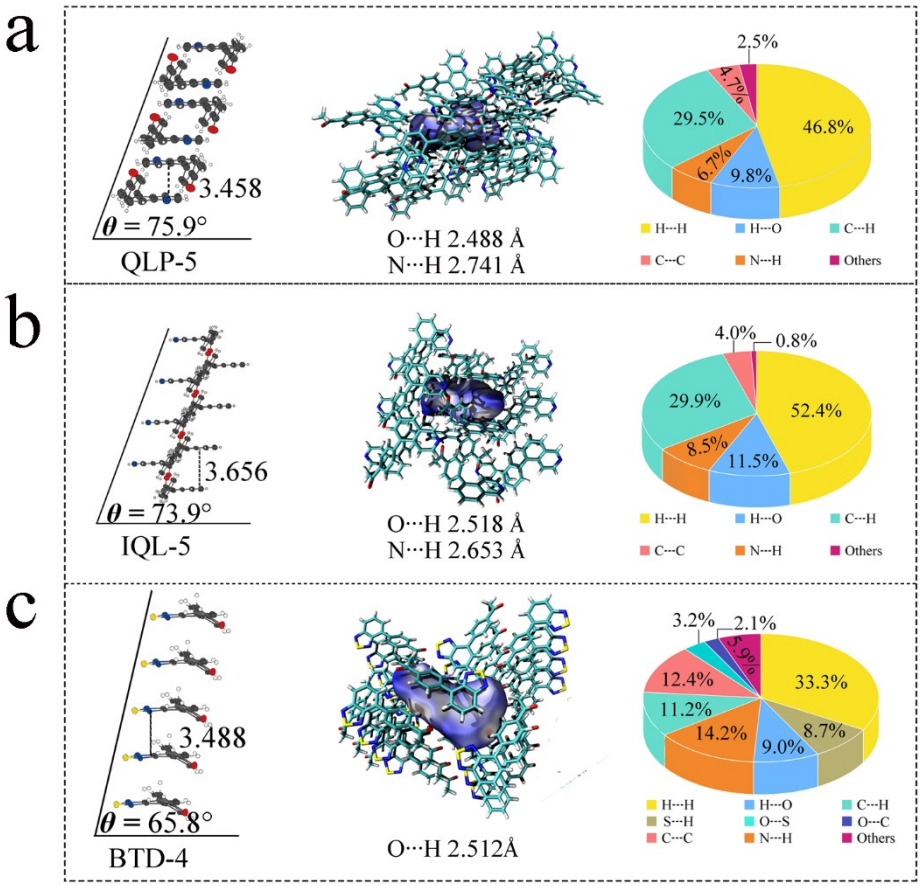

Figure S27. (left): Crystal structure. O atoms (red), N atoms (blue), C atoms (black), H atoms (white), (middle): A view of the Hirshfeld surface mapped over $d_{norm,}$ (right): The Pie-charts: Relative contributions of various intermolecular interactions to the Hirshfeld surface area of QLP-5, IQL-5 and BTD-4.

Calculation

Table S13. Calculated C−C Atomic Distances and dihedral angles of compounds and their derivatives in the ground (S_0) and excited states (S_1) based on isolated phase, calculated by the TD-DFT, ω-b97xd/Def2-TZVP level, gaussian 09 program.

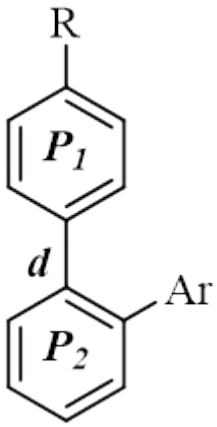

compound	State	Atomic Distance (Å) *d*	Dihedral Angle (o) P_1 and P_2
	S_0	1.47774	47.56343
QLP-8	S_1	1.47759	47.79693
	S_0	1.48940	59.26306
QLP-5	S_1	1.48070	56.35363
	S_0	1.48822	57.92384
IQL-5	S_1	1.47992	55.58285
	S_0	1.48035	36.44156
BTD-4	S_1	1.43569	16.70690
	S_0	1.48521	45.41237
QLB-8	S_1	1.47819	48.47980
	S_0	1.48464	51.67438
NTP-1	S_1	1.47797	48.78484

Table S14. Vertical excitation of single compound at the geometry of $S_{1, min}$.

Compound	Electronic states	Energy (eV)	Wavelength (nm)	Transition	Oscillator Strength (*f*)
	$S_{1, min}$ $^1(n+\sigma, \pi^*)$	3.2856	377.36	H-1 -> L (56.2%)	0.0003
QLP-8				H-1 -> L+1 (31.0%)	
	S_2 $^1(\pi, \pi^*)$	4.2662	290.62	H -> L (81.6%)	0.5174
	$S_{1, min}$ $^1(n+\sigma, \pi^*)$	3.3278	372.57	H-1 -> L (72.5%)	0.0002
QLP-5				H-1 -> L+1 (14.5%)	
	S_2 $^1(\pi, \pi^*)$	4.4217	280.40	H -> L (78.3%)	0.5376
	$S_{1, min}$ $^1(n+\sigma, \pi^*)$	3.321	373.32	H-1 -> L (73.3%)	0.0002
IQL-5				H-1 -> L+1 (14.4%)	
	S_2 $^1(\pi, \pi^*)$	4.3460	285.29	H -> L (72.6%)	0.2424
BTD-4	S_1 $^1(\pi, \pi^*)$	3.0827	402.19	H -> L (96.1%)	0.3055
	$S_{1, min}$ $^1(n+\sigma, \pi^*)$	3.3426	370.92	H-1 -> L (56.2%)	0.0002
NTP-1				H-2 -> L (22.8%)	
	S_2 $^1(\pi, \pi^*)$	4.3202	286.99	H -> L (75.7%)	0.4811
	$S_{1, min}$ $^1(n+\sigma, \pi^*)$	3.8558	321.56	H-1 -> L (60.5%)	0.0002
QLB-8				H-1 -> L+1 (26.2%)	
	S_2 $^1(\pi, \pi^*)$	4.3162	287.25	H -> L (79.6%)	0.3035

Table S15. Vertical excitation of single QLP-8 dimer in the crystal at the geometry of $S_{1,\,min}$.

Electronic states	Energy (eV)	Wavelength (nm)	Transition	Oscillator strength
S_1 $^1(\pi, \pi^*)$	2.8538	434.45	H -> L (92.7%)	0.0208
S_2 $^1(\pi, \pi^*)$	3.5889	345.47	H -> L+1 (54.0%) H-1 -> L (37.2%)	1.8289

Table S16. Vertical excitation of single QLP-8 in SMD model at the geometry of $S_{1,\,min}$.

solvent	Excited states	Energy (eV)	Wavelength (nm)	Transition	Oscillator strength
THF	$S_{1,\,min}$ $^1(n+\sigma, \pi^*)$	3.6715	337.69	H-3 -> L (41.4%) H-4 -> L (34.9%)	0.0057
	S_2 $^1(\pi, \pi^*)$	4.0753	304.23	H -> L (77.8%)	1.0649
n-hexane	$S_{1,\,min}$ $^1(n+\sigma, \pi^*)$	3.4240	362.10	H-1 -> L (61.0%) H-1 -> L+1 (26.3%)	0.0002
	S_2 $^1(\pi, \pi^*)$	4.2068	294.72	H -> L (86.3%)	0.7277
H_2O	$S_{1,\,min}$ $^1(n+\sigma, \pi^*)$	3.6717	337.68	H-3 -> L (41.2%) H-4 -> L (35.1%)	0.0057
	S_2 $^1(\pi, \pi^*)$	4.0754	304.23	H -> L (77.8%)	1.06480

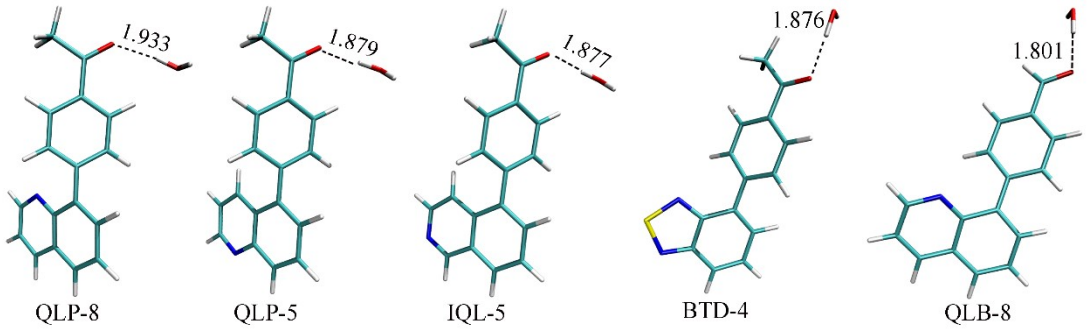

Figure S28. The water molecule and the compounds structure, calculated by gaussian 09 program under ω-b97xd/Def2-TZVP level.

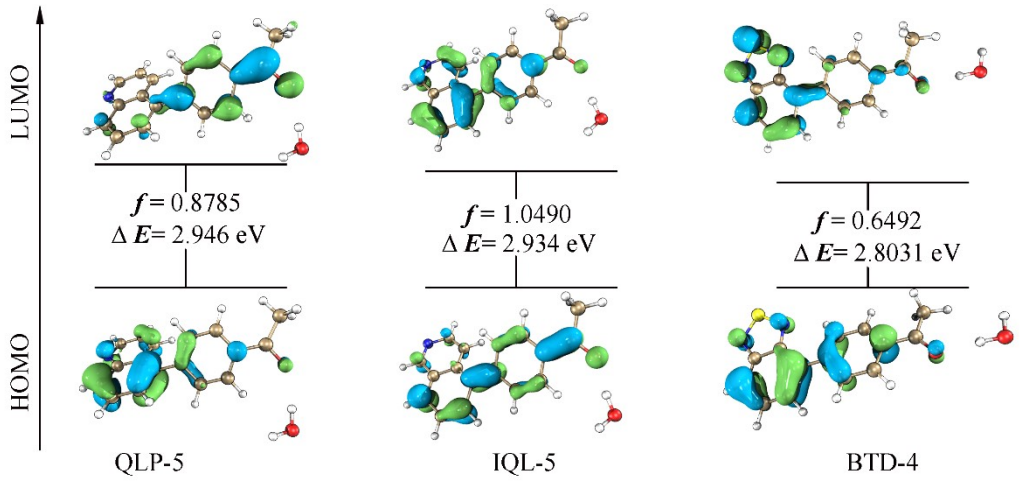

Figure S29. Optimized excited-state geometries of the water molecule and the compounds structure, calculated by TD-DFT method in gaussian 09 program under ω-b97xd/Def2-TZVP level.

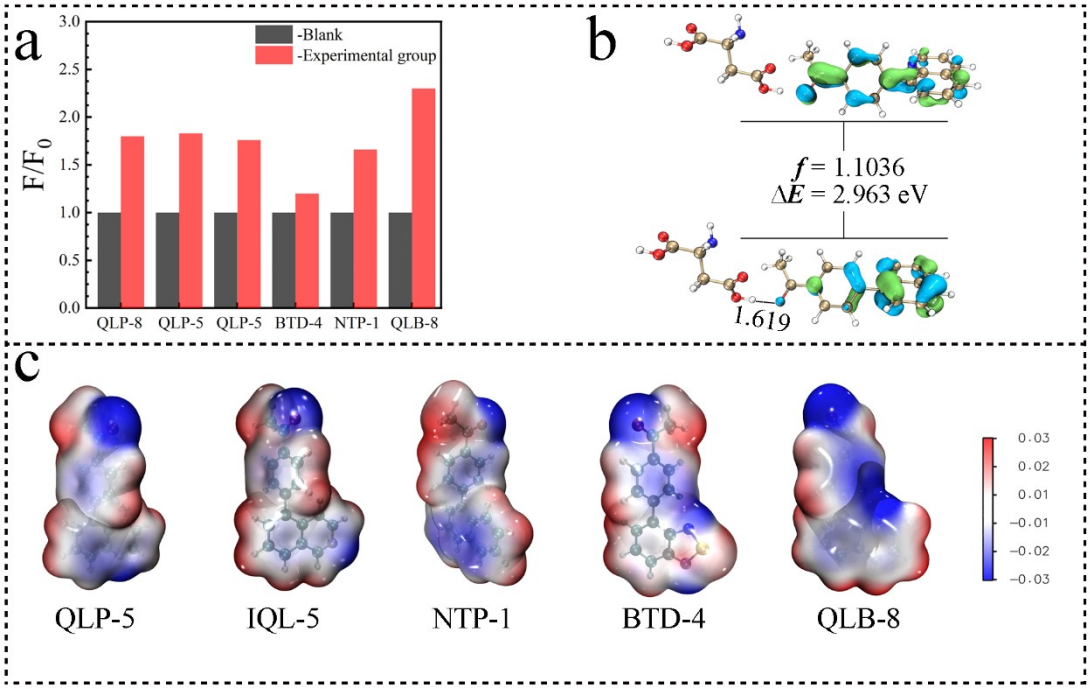

Figure S30. a. Fluorescence intensity histogram of aspartic acid detecting by different molecules. **b.** Natural transition orbitals of optimized excited-state geometries of aspartic-QLB-8 complex ware calculated by the TD-DFT method at the ω-b97xd/Def2-TZVP level, gaussian 09 program. **c.** Electrostatic potential (ESP) diagrams of QLP-5, IQL-5, NTP-1, BTD-4, QLB-8**.**

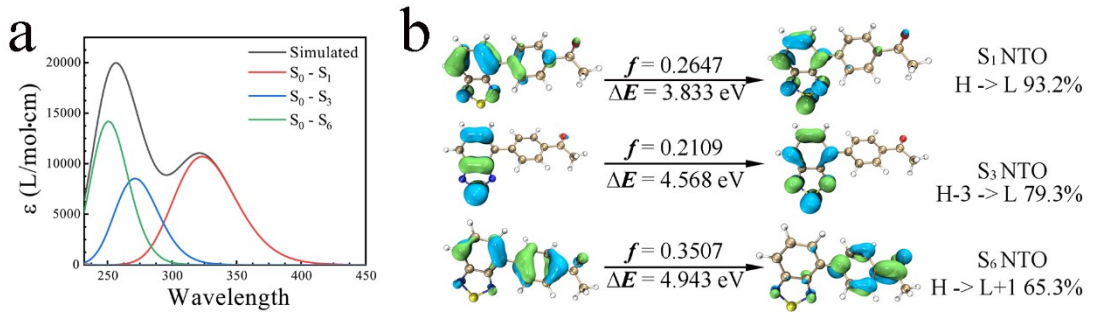

Figure S31. a. The UV–vis spectrum of BTD-4 by TD-DFT calculation. **b.** Charge distribution corresponding to different transition states**,** calculated by TD-DFT method in gaussian 09 program under ω-b97xd/Def2-TZVP level.

References

(1) Gaussian 09, Revision E.01 M. J. Frisch, G. W. Trucks, H. B. Schlegel, G. E. Scuseria, M. A. Robb, J. R. Cheeseman, G. Scalmani, V. Barone, B. Mennucci, G. A. Petersson, H. Nakatsuji, M. Caricato, X. Li, H. P. Hratchian, A. F. Izmaylov, J. Bloino, G. Zheng, J. L. Sonnenberg, M. Hada, M. Ehara, K. Toyota, R. Fukuda, J. Hasegawa, M. Ishida, T. Nakajima, Y. Honda, O. Kitao, H. Nakai, T. Vreven, J. A. Montgomery, Jr., J. E. Peralta, F. Ogliaro, M. Bearpark, J. J. Heyd, E. Brothers, K. N. Kudin, V. N. Staroverov, T. Keith, R. Kobayashi, J. Normand, K. Raghavachari, A. Rendell, J. C. Burant, S. S. Iyengar, J. Tomasi, M. Cossi, N. Rega, J. M. Millam, M. Klene, J. E. Knox, J. B. Cross, V. Bakken, C. Adamo, J. Jaramillo, R. Gomperts, R. E. Stratmann, O. Yazyev, A. J. Austin, R. Cammi, C. Pomelli, J. W. Ochterski, R. L. Martin, K. Morokuma, V. G. Zakrzewski, G. A. Voth, P. Salvador, J. J. Dannenberg, S. Dapprich, A. D. Daniels, O. Farkas, J. B. Foresman, J. V. Ortiz, J. Cioslowski, and D. J. Fox, Gaussian, Inc., Wallingford CT, 2013.

(2) Lu T, Chen F. Multiwfn: a multifunctional wavefunction analyzer[J]. Journal of computational chemistry, 2012, 33(5): 580-592.

(3) Spackman, M. A.; Jayatilaka, D. Hirshfeld Surface Analysis. CrystEngComm, 2009,11, 19-32.

(4) Dolomanov, O.V.; Bourhis, L.J.; Gildea, R.J.; Howard, J.A.K.; Puschmann, H., OLEX2: A complete structure solution, refinement and analysis program (2009). J. Appl. Cryst., 42, 339-341